Exploring the opportunities for carbon capture in modular, small-scale steam methane reforming: an energetic perspective

Exploring the opportunities for carbon capture in modular, small-scale steam methane reforming: an energetic perspective

Ishan Sharma[a], Daniel Friedrich[a], Timothy Golden[b] and Stefano Brandani[a,*]

[a] School of Engineering, The University of Edinburgh, The King's Buildings, Edinburgh EH9 3FB, UK

[b] Air Products and Chemicals, Inc., 7 Lieudit Kerguillaouet, 29920 Nevez, France

Abstract

Small-scale steam methane reforming units produce more than 12 % of all the CO_2-equivalent emissions from hydrogen production and, unlike large-scale units, are usually not integrated with other processes. In this article, the authors examine the hitherto under-explored potential to utilise the excess heat available in the small-scale steam methane reforming process for partial carbon dioxide capture. Reforming temperature has been identified as a critical operating parameter to affect the amount of excess heat available in the steam methane reforming process. Calculations suggest that reforming the natural gas at 850 °C, rather than 750 °C, increases the amount of excess heat available by about 28.4 % (at 180 °C) while, sacrificing about 1.62 % and 1.09 % in the thermal and exergetic efficiency of the process, respectively. Preliminary calculations suggest that this heat could potentially be utilised for partial carbon capture from reformer flue gas, via structured adsorbents, in a compact capture unit. The reforming temperature can be adjusted in order to regulate the amount of excess heat, and thus the carbon capture rate.

Keywords: Steam methane reforming; Small-scale; Carbon capture; Grand composite curve; Excess heat

* Corresponding author at: School of Engineering, The University of Edinburgh, The King's Buildings, Edinburgh EH9 3FB, UK. Email address: s.brandani@ed.ac.uk

Nomenclature and abbreviations

Ex_{H_2}: Material exergy associated with product H_2 stream (W)

Ex_{in}: Total input exergy (material + shaft work) (W)

LHV_{H_2}: Lower heating value of H_2 per unit mole (J/mol)

LHV_{NG}: Lower heating value of NG per unit mole (J/mol)

$\dot{m}_{H_2}$: Molar flow rate of H_2 produced (mol/s)

$\dot{m}_{NG}$: Molar flow rate of total NG input (mol/s)

$\dot{W}_{Comp+blow}$: Cumulative power input from all the compressors and blowers (W)

$\dot{W}_{Pumps}$: Cumulative power input from all the pumps (W)

η_{Ex}: Overall exergy efficiency of the SMR process

η_{Th}: Thermal efficiency of the SMR process

CCC: Committee on Climate Change

CCS: Carbon Capture and Storage

CHP: Combined Heat and Power

CO_2e: Carbon dioxide-equivalent

EOR: Enhanced Oil Recovery

EoS: Equation of State

GCC: Grand Composite Curve

ICCS: Industrial Carbon Capture and Storage

L/HP: Low/High Pressure

LMTD: Log Mean Temperature Difference

MDEA: Methyl diethanolamine

MEA: Monoethanolamine

NG: Natural Gas

SMR: Steam Methane Reforming

TSA: Temperature Swing Adsorption

VOC: Volatile Organic Compound

V/PSA: Vacuum/Pressure Swing Adsorption

1. Introduction

In the long term, the Paris agreement aims to limit the rise in global average temperature to well below 2 °C above the pre-industrial era levels. Even before signing the agreement, the United Kingdom (UK), along with several other European Union (EU) countries have made significant progress towards reducing their carbon dioxide-equivalent (CO_2e) emissions. For instance, in 2008, the UK government passed the Climate Change Act, with an aim to reduce their CO_2e emissions by at least 80 % from the 1990 baseline level. The UK had already achieved a 41 % reduction in their net CO_2e emissions by 2016, even though the economy grew by 60 % over the same duration (Department for Business, 2018). However, since 2012, three-quarters of the reduction has been due to a decrease in coal usage in the power sector (Department for Business, 2018). Further scope of reduction in CO_2e emissions is limited, even if all the coal-fired power plants are closed (Committee on Climate Change (UK), 2017). In fact, in the case of the UK, the transport sector (26 % of the total) has become the largest emitter, surpassing the energy sector (25 %) in 2016. Other significant sectors contributing to the total CO_2e emissions include business and industrial (17 %), residential (14 %) and agriculture (10 %) (Department for Business, 2018). Carbon Capture and Storage (CCS) is a crucial strategy to reduce the carbon emissions where renewable sources cannot readily replace fossil fuels, especially in the industrial sector. A Committee on Climate Change (CCC) report to the UK parliament identifies CCS as a vital strategy to meet the UK government's target of reducing CO_2e emissions to at least 80 % of the 1990 baseline level (Committee on Climate Change (UK), 2017). The report expects CCS to significantly contribute to emission reductions in the industrial and power sector.

Hydrogen (H_2) is an essential raw material used to produce critical commodity chemicals such as ammonia and methanol. H_2 is also used in large quantities for desulphurisation of oil refinery products. Additionally, the proponents of the 'hydrogen economy' advocate H_2 use in applications ranging from transportation, residential and commercial heating, stationary power generation and energy storage. If the hydrogen economy ever becomes a reality, there are primarily two scales at which H_2 could be produced, viz. large and small.

Large-scale H_2 production would involve the centralised production of H_2 in large facilities, supported by a dedicated distribution network. Since, at present, the H_2 distribution network has limited coverage, it will require a significant investment to develop the necessary infrastructure. The existing Natural Gas (NG) distribution network may or may not be suitable for H_2 distribution. For example, in the UK, all gas pipelines within 30 meters of buildings are currently being replaced with polyethylene pipes, considered to be suitable for transporting pure H_2 (Northern Gas Networks, 2016). This will still leave the remaining network unsuitable for H_2 transport. It will take some time before the network is completely upgraded. In addition, the pipes are still in use for NG, so not available unless wholly switched. The other alternative is to transport the hydrogen via trucks, trailers or ships which would also imply significant additional costs. Currently, the majority of H_2 production is at a large-scale for industrial applications, through the process of Steam Methane Reforming (SMR) (Lemus & Duart, 2010). Electrolysis of water is an alternative process to produce H_2 at a relatively large-scale and with a small carbon footprint; provided that the electricity is generated from a low-carbon source. For large-scale H_2 production, multiple electrolyser assemblies would probably be needed, as the maximum capacity of an installed electrolyser in Europe is just 2,875 Nm^3/h (H_2 Tools, 2013). With the NG prices being low and relatively stable, electrolysis is typically expected to

be more expensive than SMR for large-scale H_2 production, at least in the near future (Lemus & Duart, 2010; Ekins et al., 2010).

H_2 is produced at a small-scale (up to a few thousand Nm^3/h) when a consumer does not have access to an H_2 distribution network. Industrial applications of small-scale SMR range from food processing, glass, metals, semiconductor manufacturing, and analytical laboratory instrumentation (Department of Energy (US), 2013). In the UK, out of the twelve merchant H_2 production units (i.e., standalone units, not part of an industrial complex), eleven could be classified as small-scale (H_2 Tools, 2013). The total CO_2e emissions from these small-scale units amount to at least 12 % of the total CO_2e emissions from H_2 production in the UK. The number of small-scale SMR plants is only going to increase as H_2 adoption increases with a hydrogen economy becoming a reality. Due to economies of scale, the cost of H_2 production at large-scale is typically lower than that at small-scale. The small-scale units often come in modular and standardised design, which is essential to keep the capital costs low. If there is enough demand, the units could be produced in bulk, thereby making them cheaper still. Typically, it is expected that at small-scale, the cost of H_2 production by SMR is lower than that by electrolysis (Department of Energy (US), 2013; Ekins et al., 2010). However, electrolysis can be competitive if there is a cheap source of electricity available (Ekins et al., 2010).

A small-scale SMR process differs from a large-scale SMR process with regard to the operating conditions and the overall system configuration. The reforming conditions are less severe in small-scale SMR to limit the need for specialised materials for construction. A small-scale SMR unit also has fewer unit operations to keep the system compact. As the SMR process has excess heat available, the large-scale SMR plants generally have a provision for steam export. While, on the other hand, small-scale SMR units come as a ‘plug-and-play’ device and are not usually integrated with any other process plant on-site. This offers an interesting opportunity to utilise the excess heat, in order to capture at least a part of the total carbon dioxide (CO_2) generated during the conversion of NG into H_2.

The SMR process is considered a ‘low hanging fruit' for carbon capture. The shifted syngas and H_2 Pressure Swing Adsorption (PSA) tail gas contain almost half of the total CO_2 produced in the process at relatively high partial pressures. The additional penalty of carbon capture at such a high partial pressure is expected to be significantly lower than what would have been incurred in case of capture from a conventional power plant. The scientific community and corporations have thus far mostly focussed on CCS in large-scale SMR. For example, Soltani et al. (2014) have analysed the favourability of CO_2 capture at different locations, within a large-scale SMR plant, using an empirical factor. They have defined this factor as the product of CO_2 partial pressure, concentration and the fraction of CO_2 captured. Soltani et al. (2014) have not delved extensively into the energetic aspects of carbon capture in SMR. It will be later illustrated in this article that analysing the SMR process from an energetic point of view is crucial to ensure economical CO_2 capture. Meerman et al. (2012) have looked into the techno-economic feasibility of CO_2 capture from a large-scale merchant SMR unit, using commercially available ADIP-X technology. The ADIP-X technology, supplied by Shell, uses a methyl diethanolamine (MDEA) solution, with piperazine as an accelerator, to chemically absorb the CO_2. To provide the energy needed for solvent regeneration, Meerman, et al. (2012) have used a separate Combined Heat and Power (CHP) unit; however, the additional CO_2 emitted from the CHP unit is not captured. Recently, Amec Foster Wheeler has conducted

another study to assess the techno-economic feasibility of deploying CCS in a large-scale merchant SMR plant. The study considers different alternatives to capture CO_2, from different locations within a large-scale SMR process (Collodi et al., 2017). The CO_2 capture technologies discussed in the study are chemical absorption in MDEA, monoethanolamine (MEA); cryogenic and membrane separation. Where applicable, a back pressure turbine is used to meet the solvent regeneration requirements by generating Low Pressure (LP) steam from exported High Pressure (HP) steam.

Industrial CCS demonstrations in large-scale SMR have been summarised in Table 1. Carbon capture from the reformer flue stack has not been implemented in any of the industrial demonstration plants. This implies that at least half of the total CO_2 emissions from these plants is still not being captured.

Table 1: Summary of the industrial demonstrations of CO_2 capture in large and small-scale SMR units.

CO_2 capture demonstration projects for large-scale SMR		
Project	**Operator**	**Key attributes**
Port Arthur project (US)	Air Products and Chemicals	• First large-scale CCS application in SMR • Supported through the US Department of Energy's Industrial Carbon Capture and Storage (ICCS) program • Vacuum Swing Adsorption (VSA) process to capture a million tonnes of CO_2 per year from the shifted syngas • captured CO_2 is used for Enhanced Oil Recovery (EOR) (Baade et al., 2012)
Quest CCS project (Canada)	Shell	• ADIP-X technology to capture a million tonnes of CO_2 per year from the shifted syngas since 2015 (Cap-Op Energy, 2015)
Tomakomai project (Japan)	Japan CCS Co. Ltd.	• Activated MDEA-based solvent to capture a hundred thousand tonnes of CO_2 per year from the PSA tail gas since 2015 (Tanaka et al., 2017)
Port- Jérôme project (France)	Air Liquide	• Cryocap™ cryogenic process captures about a 100,000 tonnes of CO_2 per year from the PSA tail gas (Air Liquide, 2015) • Claims to be the only SMR-based carbon capture process capable of increasing H_2 production while limiting the CO_2 emissions (Air Liquide, 2015)
CO_2 capture demonstration projects for small-scale SMR		
Haneda hydrogen station (Japan)	Tokyo Gas Co.	• Captured the CO_2 through liquefaction of PSA tail gas • Operated from 2010 to 2016 (IEA-HIA, 2012)

The European project named HY2SEPS-2 has looked into the design of hybrid separation processes, combining membrane and PSA process, for H_2 separation in small-scale SMR (FCH JU, 2013). The project evaluated different configurations of the hybrid separation process in order to achieve a higher H_2 recovery, for the same H_2 purity. Such a hybrid separation process

also has the potential of co-producing a CO_2 rich stream for sequestration (CORDIS, 2015). One of the technology providers of small-scale SMR, viz. HYGEAR was also a part of the HY2SEPS-2 project. As part of the project, Silva et al. (2013) characterised the CuBTC MOF for H_2 separation from the shifted syngas stream. At small-scale, the Haneda hydrogen station in Tokyo is the only carbon capture demonstration unit for SMR. Table 1 summarises the key attributes of the Haneda carbon capture facility. For H_2 production capacities less than 500 Nm^3/h, CCS is not expected to be economically viable, unless there is demand for CO_2 nearby or the transport costs are low (Schjolberg at al., 2012). Needless to say, if a small-scale SMR unit already has access to CO_2 distribution infrastructure, there lies a favourable opportunity to reduce the carbon footprint of the process significantly. This might be true when an industrial cluster contains the small-scale SMR.

Several vendors supply small-scale, on-site SMR based H_2 production units, including Air Products and Chemicals, Linde gas, Mitsubishi, and HYGEAR. The small-scale SMR units are usually supplied as a modular unit, fitted inside a shipping container. For the small-scale SMR units, a small physical footprint of the CO_2 capture unit is an essential requirement; the compactness of the small-scale units is one of their key features. Due to their large physical footprint, absorption-based CO_2 capture solutions are not expected to be feasible for small-scale SMR. Abanades J.C. et al. (2015) also emphasise the need to intensify the adsorption-based CO_2 capture units to drive down the CO_2 capture costs. Intensification is key to reduce adsorbent requirements and capital costs. Structured adsorbent-based cyclic processes, characterised by their high productivity (amount of feed processed per unit system volume), can be a viable alternative to conventional absorption-based solutions. Conventional adsorption processes consist of multiple packed columns, filled with pelleted adsorbent. Adsorption columns, packed with pelleted adsorbents, tend to suffer from significant pressure drops at high flow rates (Ruthven and Thaeron, 1997). Alternate adsorbent structures have thus been investigated as an alternative to pelleted adsorbents. Examples of such structures include; monoliths, laminates, foams and fabric structures (Rezaei and Webley, 2010). Usually, the active adsorbent is coated onto these structures; although direct extrusion is possible for some of the adsorbents. Such structured adsorbents do not suffer from potential fluidisation due to their immobilisation onto the fixed structure. If appropriately designed, structured adsorbents can exhibit a lower pressure drop per unit length, along with higher mass and heat transfer rates than their pelleted counterparts. Structured adsorbents have recently found application in CO_2 capture from flue gas (Miller, 2016).

In the past, multi-port rotary valves and rotary adsorption assemblies have also been used in the commercial adsorption-based separation process to reduce physical footprint. Multi-port rotary valves can significantly reduce the number of valves and the extent of piping required by the process. Rotary adsorption assemblies find applications in dilute gas separation applications, like air de-humidification, Volatile Organic Compound (VOC) removal, etc. Rotary adsorption assemblies often consist of a rotating wheel which is composed of structured channels and coated with an active adsorbent. Fixed compartments or ports at the two ends of the wheel divide it into different segments. Because of leakage concerns between the compartments, rotary beds are usually only used in Temperature Swing Adsorption (TSA) applications. As the wheel rotates at a fixed rotational speed, a single structured channel undergoes different steps of the TSA process. The review article by Rezaei and Webley (2010) covers the subject matter extensively.

In this paper, the authors have analysed a typical base-case, small-scale, SMR process from the energetic and exergetic point of views. The authors have used a commercial process simulator (UniSim) to model the process and highlighted the inherent flexibility that the small-scale SMR process offers concerning CO_2 capture. Additionally, since physical space availability is often a constraint for small-scale SMR units, a preliminary assessment of the likely physical footprint of a structured adsorbent-based TSA capture unit has been estimated. To the best of our knowledge, such a detailed analysis of a small-scale SMR process is not present in the existing open literature, and the authors intend to fill this research gap. In the immediate future, this would provide a useful base-case for implementing CCS in small-scale SMR units, already having access to a CO_2 distribution network.

2. Small-scale SMR

Figure 1 shows the typical processing steps in an SMR process. SMR primarily involves the reaction of methane and steam, through an endothermic reaction (1), in order to produce hydrogen and carbon monoxide. Rather than pure methane, NG is the typical feedstock used in SMR plants. It is for this reason that some large-scale SMR plants may also have a pre-reforming step to react higher alkanes and steam, according to reaction (2). Mercaptan compounds are often added to NG to aid in leakage detection. As the catalysts used in the SMR process are susceptible to sulphur compounds, the NG is desulphurised first, before sending it to the reformer.

$$CH_4(g) + H_2O(g) + Heat \leftrightarrow CO(g) + 3H_2(g) \quad (1)$$

$$C_nH_{(2n+2)}(g) + nH_2O(g) + Heat \leftrightarrow nCO(g) + (2n+1)H_2(g) \quad (2)$$

CH_4: Methane

H_2O: Water/Steam

CO: Carbon monoxide

$C_nH_{(2n+2)}$: Generic Alkane in NG, n>1

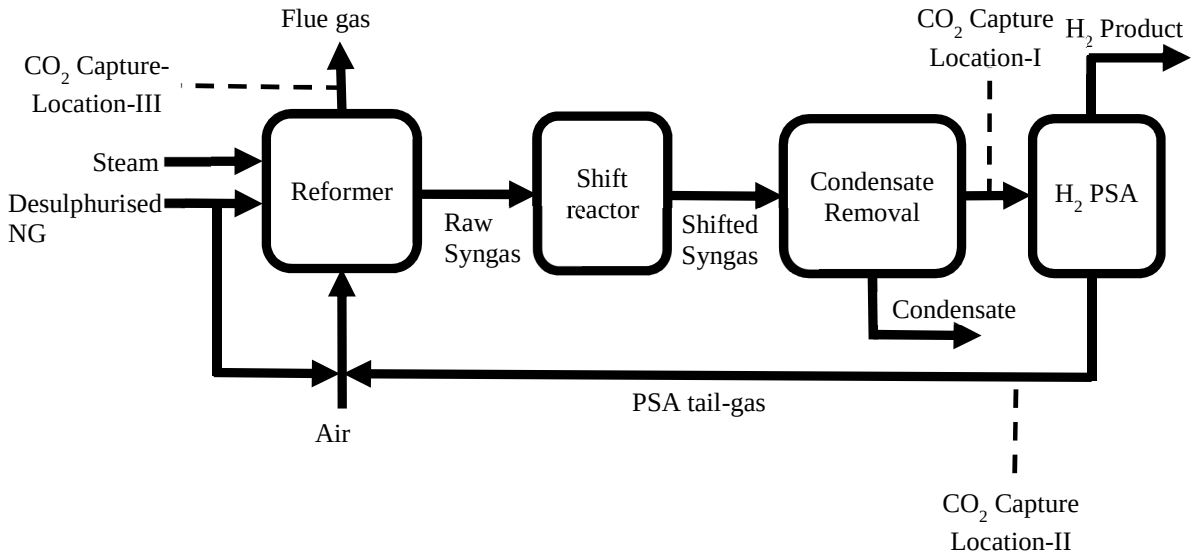

Figure 1: Typical processing steps in SMR

Reforming:

The reformer is an externally-fired, tubular furnace. The de-sulphurised NG stream is mixed with steam, before being fed to the reformer. The reaction mixture passes through multiple tubes which are filled with a nickel-based catalyst (Maxwell, 2005). The heat required for the endothermic reforming reaction comes from burning fuel (typically, a mixture of NG and waste streams). Reforming temperature and pressure ranges from 700 to 850 °C and 3 to 25 bar, respectively (IEA-HIA, 2006).

Reforming is performed at moderate pressures in large-scale operations, even though high temperature and low pressure favour the forward reaction in (1). The purpose is to limit the downstream equipment sizes and the H_2 pressurisation costs. Due to the expensive materials needed for high temperature and pressure operation, a lower reforming pressure and temperature are desirable for small-scale operations (Ogden, 2001). Apart from (1) and (2), reactions (3), (4) and (5) also occur in the reformer.

$$CO(g) + H_2O(g) \leftrightarrow CO_2(g) + H_2(g) + Heat \quad (3)$$

$$CH_4(g) + Heat \leftrightarrow C(s) + 2H_2(g) \quad (4)$$

$$2CO(g) \leftrightarrow CO_2(g) + C(s) + Heat \quad (5)$$

Reactions (4) and (5) result in coke deposition on the catalyst, thereby leading to its de-activation. Excess steam is fed into the reformer to promote reactions (1), (2) and (3) over (4) and (5). The typical range for steam to methane ratio (mole basis) is 2.5 to 4.5 (Maxwell, 2005). The product gas from the reformer is known as raw syngas, and it mainly consists of a mixture of H_2, CO, CO_2, H_2O and unreformed CH_4.

Water-gas shift:

The exothermic water-gas shift reaction involves the conversion of carbon monoxide to H_2, as shown in (3). Since the water gas shift reaction is exothermic, a lower reaction temperature is preferred to increase the carbon-monoxide conversion at equilibrium. Typically, a trade-off between a higher conversion and a higher reaction rate is achieved in large-scale SMR plants by carrying out the reaction in two reactors in series. For small-scale SMR units, where the aim is to make the system compact, a single stage shift is a preferred alternative to the conventional two-stage shift, as reflected from most of the commercial small-scale SMR technologies (Air Products and Chemicals, Inc, 2018; The Linde Group, 2018; Mitsubishi Kakoki Kaisha, Ltd., 2018).

Hydrogen purification by PSA:

For high H_2 purity requirements, modern SMR plants are equipped with a PSA unit. The PSA unit can produce a high purity hydrogen stream (typically>99.99 % by mole) from the shifted syngas stream (Hamelinck & Faaij, 2002). The shifted syngas stream is cooled down to near ambient temperature conditions. The water, thus condensed, is separated in a flash tank. Any remaining water is also typically removed by using a guard bed for the H_2 PSA unit. The patent by Wagner (1969) is the first patent filed for PSA-based H_2 purification, making use of two different adsorbent layers. The article by Sircar & Golden (2000) provides a comprehensive review of commercial H_2 PSA units in use today that are capable of producing high purity hydrogen. Sircar & Golden (2000) divided the commercial H_2 PSA processes into two categories, viz. processes that only produce pure hydrogen and those which can simultaneously provide both pure hydrogen and CO_2 streams. The UOP's Polybed™ and Toyo Engineering Corporation's Lofin™ processes fall in the first category, while the Gemini™ process, from Air Products and Chemicals, falls in the second category. Recently, Shi et al. (2018) have also proposed a two-stage PSA/VSA system to simultaneously produce both H_2 and CO_2 streams from the shifted syngas. The PSA unit is similar to the conventional layered H_2 PSA, while a VSA unit employing silica gel as an adsorbent is used to produce a CO_2 stream with 95 % purity and 90 % recovery.

Carbon capture locations:

Potential locations for carbon capture by adsorption include the shifted syngas (after condensate removal) (location I), or the H_2 PSA tail gas (location II). Another opportunity to capture CO_2 is from the reformer flue gas (location III), either with or without CO_2 capture from locations I or II. It is relatively cheap to capture CO_2 from locations I and II, as the partial pressure of CO_2 is relatively higher than in the flue gas (location III).

3. Process flowsheet and modelling assumptions

Figure 2 depicts the process flow diagram of the small-scale SMR process modelled in UniSim. Table 2 lists the physical state and composition of the NG used in the modelling. The NG has been assumed to be free of any sulphur. The assumption does not affect the results to any appreciable extent as the amount of H_2 consumed in the hydrodesulphurisation step is insignificant, as compared to the total H_2 produced. Table 3 lists the different process sections, along with the assumptions made concerning the operating conditions of the base-case, smallscale SMR process. The assumptions are based on the typical design data available in the open literature for small-scale, on-site SMR units, supplied by different technology licensors. The UniSim model uses the Peng-Robinson Equation of State (EoS). The reactions in the reformer and shift reactor have been assumed to reach equilibrium conversion. The H_2 PSA has been modelled using a component splitter in UniSim, by specifying H_2 purity and recovery.

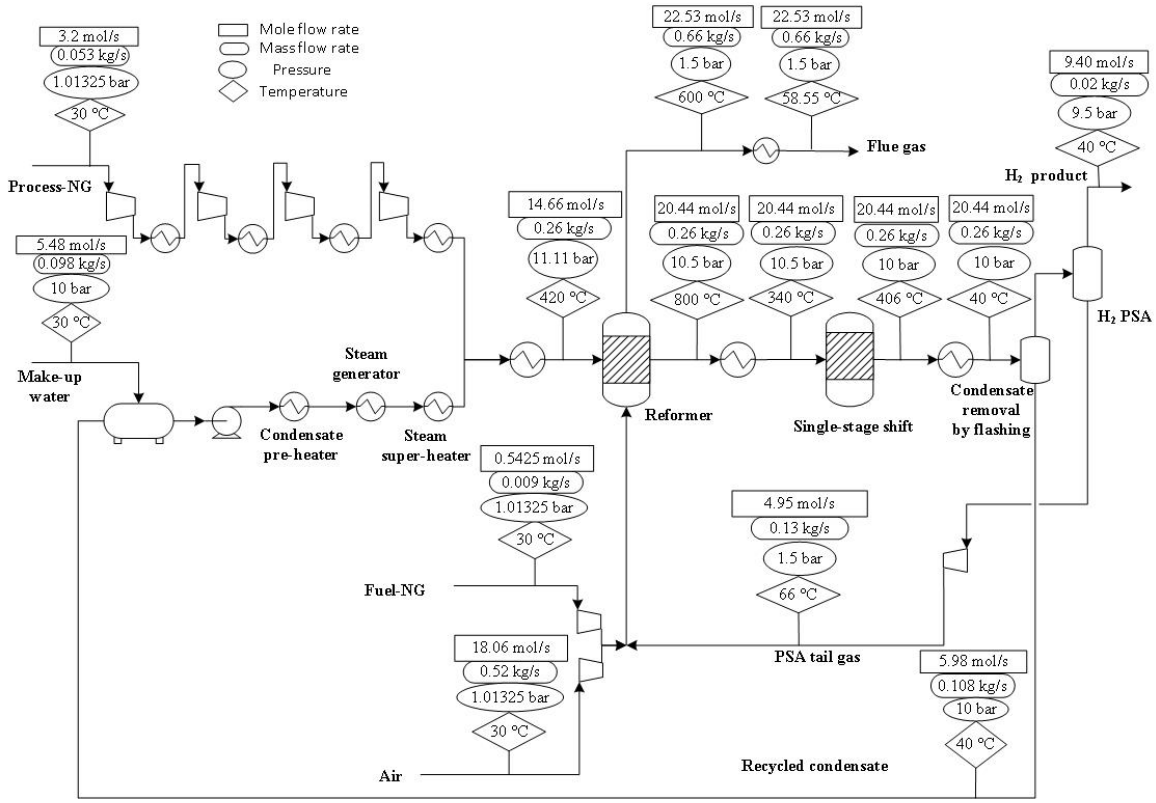

Figure 2: Process flow diagram for the base-case, small-scale SMR process (reforming temperature: 800 °C)

Table 2: NG composition used in the modelling

Component	**Mole fraction**
Methane (CH_4)	0.9623
Ethane (C_2H_6)	0.0283
Propane (C_3H_8)	0.0013
n-Butane(C_4H_{10})	0.0001
i-Butane(C_4H_{10})	0.0001
n-Pentane(C_5H_{12})	0
i-Pentane(C_5H_{12})	0
n-Hexane(C_6H_{14})	0
Nitrogen(N_2)	0.0055
Carbon dioxide(CO_2)	0.0024
Water (H_2O)	0
Pressure	1.01325 bar
Temperature	30 °C

Table 3: Process sections and modelling assumptions for base-case, small-scale SMR process (reforming temperature: 800 °C)

Process section	**Base-case modelling Assumptions**	**Remarks**
Plant Capacity	Small-scale SMR ~ 800 Nm^3/h H_2	
NG pressurisation train	A four-stage compressor, with intercoolers. The NG is compressed from atmospheric pressure, in equal pressure ratios. Pressure ratio: 1.86	
Reforming	Steam-to-carbon ratio (molar): 3.5 Process-side inlet temperature (tube): 420 °C Process-side (tube) outlet temperature or reforming temperature: 800 °C Process-side (tube) outlet pressure: 10.5 bar Flue gas outlet temperature from the reformer: 600 °C Excess air used for combustion: 30% Fuel+Air mixture inlet temperature: 50 °C	The flue gas exit temperature has been taken to be substantially higher than the process-side inlet to ensure a high Log Mean Temperature Difference (LMTD) and hence, a lower convective heat transfer area.
Shift	Number of adiabatic shift stages: One Syngas inlet temperature: 340 °C	
PSA unit	H_2 PSA with an aim to ensure high purity and recovery of H_2. H_2 product purity: 99.999% H_2 Recovery: 85%	

4. Thermal efficiency for the base-case, small-scale SMR

The thermal efficiency of an SMR process can be evaluated based on the first law of thermodynamics, as shown in Eq. (5) (Simpson and Lutz, 2007). The thermal efficiency for the base-case, small-scale SMR process has been calculated to be 73.3 %.

$$\eta_{Th} = \frac{\dot{m_{H_2}} LHV_{H_2}}{\dot{m_{NG}} LHV_{NG} + \dot{W}_{Comp+blow} + \dot{W}_{Pumps}} \quad (5)$$

Where,

η_{Th}: Thermal efficiency of the SMR process

$\dot{m_{H_2}}$: Molar flow rate of H_2 produced (mol/s)

LHV_{H_2}: Lower heating value of H_2 per unit mole (J/mol)

$\dot{m_{NG}}$: Molar flow rate of total NG input (mol/s)

LHV_{NG}: Lower heating value of NG per unit mole (J/mol)

$\dot{W}_{Comp+blow}$: Cumulative power input from all the compressors and blowers (W)

$\dot{W}_{Pumps}$: Cumulative power input from all the pumps (W)

The thermal efficiency does not capture the difference in 'quality' of different energy terms; pinch and exergy analysis should rather be used to account for this difference. The following section covers these topics in detail.

5. Pinch and exergy analysis

Figure 3 shows the Grand Composite Curve (GCC) of the base-case, small-scale SMR process. The horizontal section in the GCC represents the generation of reforming steam. The part of the GCC, below the horizontal section, represents the amount of excess heat available at different temperature levels. In large-scale SMR plants, the excess heat is used to generate steam which can either be exported or utilised in a steam turbine to supply a part of the electricity required for plant operation. In small-scale SMR plants, this excess heat could potentially be utilised for carbon capture, as they are not usually thermally integrated with other process plants on-site. The reforming temperature is one of the most critical parameters to regulate the amount of excess heat (Grover, 2012), as evident from the GCCs at reforming temperatures of 750, 800 (base-case) and 850 °C. Table 4 summarises the critical performance parameters obtained for the three cases.

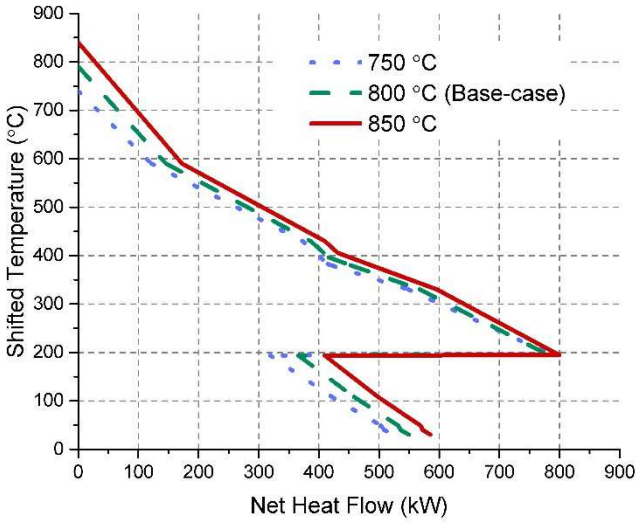

Figure 3: GCCs corresponding to different reforming temperatures

Table 4: Small-scale SMR performance at different reforming temperatures

	Reforming Temperature		
	750 °C	**800 °C (Base-case)**	**850 °C**
Process-NG (mol NG/mol H_2)	0.383	0.340	0.319
Reforming Steam (mol H_2O/mol H_2)	1.372	1.218	1.143
Fuel-NG (mol NG/mol H_2)	0.012	0.058	0.083
Total NG (mol NG/mol H_2)	0.395	0.398	0.402
CO_2 in shifted syngas (mol CO_2/mol H_2)	0.274	0.264	0.258
Total CO_2 emissions (in the absence of any CO_2 capture from shifted syngas) (mol CO_2/mol H_2)	0.405	0.408	0.412
Thermal efficiency (η_{Th})	0.740	0.735	0.728

The thermal efficiency of the process increases with reducing reforming temperature, also indicated by the decreasing total-NG consumption with reducing reforming temperature. In the context of H_2 production, without any consideration for CO_2 capture, operating at lower reforming temperature would be preferred. However, too low a reforming temperature might result in kinetic limitations. It is interesting to explore the optimum reforming temperature, in the context of H_2 production with CO_2 capture. As reported in Table 4, a reduction in reforming temperature also leads to an increase in steam demand. The rise in steam consumption is also evident from the length of the horizontal segment on the GCCs. This, coupled with the reduction in fuel-NG demand, reduces the amount of recoverable heat from the flue gas. The reduction in fuel-NG demand is due to a higher process-NG being recycled as fuel, due to lower conversion in the reformer.

Due to a fall in thermal efficiency, amounting to 1.62 %, the total CO_2 emissions increase by about 1.65 % when the NG is reformed at 850 °C, rather than 750 °C. The amount of CO_2 available at a higher partial pressure (in shifted syngas) also decreases by about 5.7 %. However, at the same time, the amount of excess heat available in the process at 180 °C increases by about 28.4 %. This inherent flexibility within the SMR process offers an opportunity to substantially increase the energy available for CO_2 capture, with only a marginal decrease in process performance. A TSA process could use the excess heat for carbon capture from reformer flue gas. However, the reforming temperature needs to be adjusted, in order to ensure that just enough excess heat is available and the fall in process efficiency is minimum. Increasing the reforming temperature would also require an increase in the size of the unit operations, due to the rise in the volume of gas flow through the process. However, this alternative is better than having to install an additional unit operation in order to generate the required energy for CO_2 capture.

An exergy analysis for the small-scale SMR process, at different reforming temperatures, yields similar results. The exergy associated with different material and work streams have been calculated to perform the exergy balance across different sections of the small-scale SMR process. The exergy related to the material flow consists of physical, chemical and mixing exergies, and have been calculated as per the methodology proposed by Hajjaji et al. (2012). The overall exergy balance gives the total exergy lost or unutilised during heat transfer. Figure 4 depicts the exergy flow for the small-scale SMR processes, corresponding to reforming temperatures of 750, 800 and 850 °C, respectively.

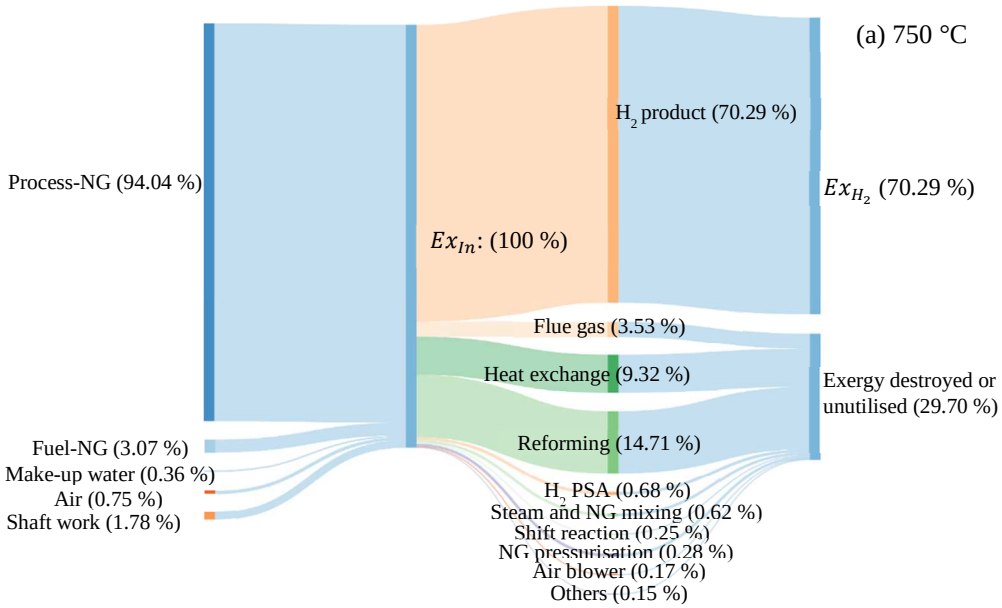

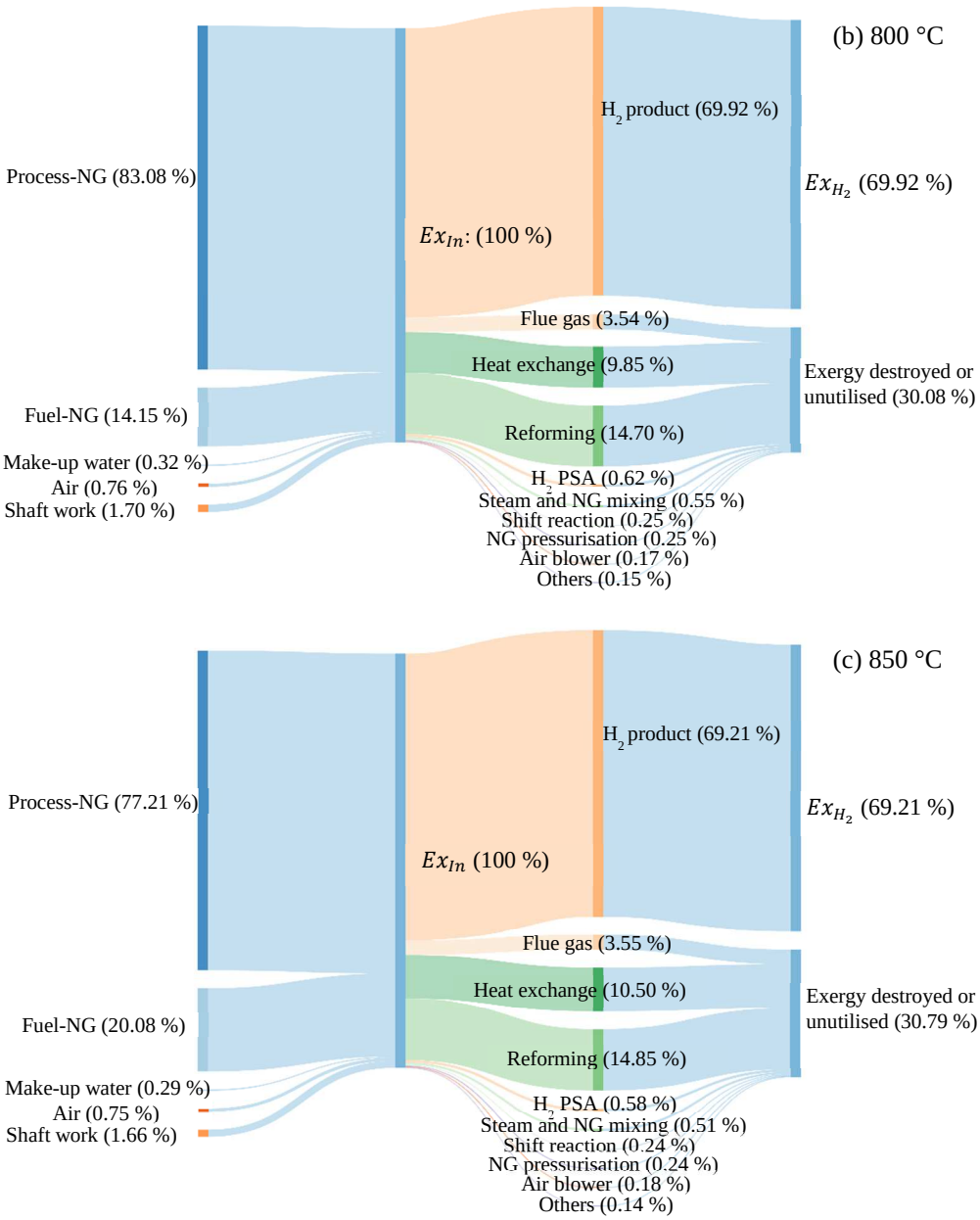

Figure 4: Exergy flow in the small-scale SMR process for reforming temperatures of (a) 750, (b) 800 and (c) 850 °C

As discussed earlier, with increasing reforming temperature, the demand for process-NG decreases, while that for fuel-NG increases. An increase in reforming temperature also results in an increase in unutilised exergy associated with heat exchange. The slight (1.09 %) reduction in overall exergy efficiency(η_{Ex}), defined here by Eq. (6), is due to the corresponding increase in the specific consumption of total-NG (as reported in Table 4). However, a part of the unutilised exergy associated with heat exchange could be used to capture a portion of the total CO_2 emissions.

$$\eta_{Ex} = \frac{Ex_{H_2}}{Ex_{in}} \tag{6}$$

Where,

Ex_{H_2}: Material exergy associated with product H_2 stream (W)

Ex_{in}: Total input exergy (material + shaft work) (W)

For small-scale SMR process, the next step is to design a CO_2 capture process with a small physical footprint, while consuming the lowest energy possible. The following section details a preliminary assessment of the likely energetic and physical footprint requirements, for a structured adsorbent-based TSA unit to capture CO_2 from reformer flue gas.

6. Structured adsorbent-based CO_2 capture in small-scale SMR: a preliminary assessment

The CO_2 partial pressure in shifted syngas (location I), H_2 PSA tail gas (location II) and reformer flue gas (location III) are about 1.7, 0.75 and 0.20 bar, respectively. A rapid cycle VSA process is expected to be one of the suitable options for carbon capture from shifted syngas or H_2 PSA tail gas, due to the higher partial pressure of CO_2 in these streams. A detailed analysis of the rapid cycle VSA unit is outside the scope of this contribution. Carbon capture from shifted syngas (or H_2 PSA tail gas) also has the positive side-effect on the fuel-NG consumption. The reduction in fuel consumption is due to a lower amount of inerts in the H_2 PSA tail gas; this also results in a fall in the total amount of CO_2 generated within the process. However, the electrical power required for the VSA unit would have to be imported from the grid. Because of the extremely low partial pressure of CO_2 in the reformer flue gas, a TSA process can be competitive with a VSA process. An added advantage of using a TSA process is that it can directly utilise the excess heat available within the SMR process for adsorbent regeneration.

For the preliminary assessment, it has been assumed that a VSA process captures 90 % of the CO_2 content in the shifted syngas. The aim is to verify whether the excess heat in a small-scale SMR unit could be used to meet the energy requirements of a TSA unit to capture the remaining CO_2 (approximately 40% of the total) from reformer flue gas. The TSA unit is assumed to consist of a rotary wheel made out of corrugated channels, like the ones reported by Mohammadi (2017) (Figure 5). The structure includes a conductive support material (assumed to be aluminium (Al) in this study), coated with commercial Zeolite 13X; as it has been previously reported to be one of the best candidates for carbon capture from flue gas (Boot-Handford et al., 2014). The rotary wheel has been assumed to be divided into two segments, viz. adsorption and desorption. In the desorption segment, a heated stream of product CO_2 is used to regenerate the adsorbent at a temperature of 150 °C.

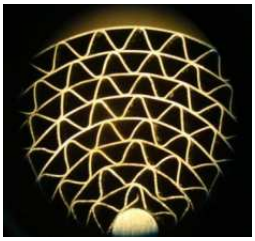

Figure 5: The rotary wheel is assumed to be composed of corrugated channels, similar to those shown in the figure (image from Mohammadi, 2017)

The UniSim model for the base-case (reforming temperature of 800 °C), provides the flow rate and concentration of CO_2 in the flue gas. For the sake of simplicity, the mass transfer kinetics (rate of adsorption/desorption) have been assumed to be fast; this ensures an almost instantaneous adsorption equilibrium between the bulk fluid phase and adsorbed phase. Table 5 reproduces the channel and adsorbent layer characteristics, as reported in Mohammadi (2017). Table 6 summarises the additional assumptions, along with the expected space and energy requirements of the TSA unit.

Table 5: Channel and adsorbent layer characteristics (Mohammadi, 2017)

Shape of an average free channel	Sinusoidal	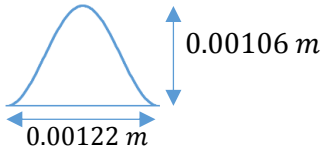
Adsorbent layer thickness	0.000031 m	
Metal foil thickness	0.000052 m	
Average bulk porosity of an individual channel	0.74	The fraction of the free cross-sectional area in the total (support material, adsorbent and free) cross-sectional area
Adsorbent	Zeolite 13X	
Adsorbent layer density	1110 kg/m^3	
Adsorbent layer porosity	0.54	
Adsorbent bulk loading density	151 kg/m^3	

Table 6: Critical assumptions and results for the preliminary assessment

Assumptions		
Total cycle time for the TSA cycle	600 s	$1/10^{th}$ of the wheel's rotation in 60 s or a rotation frequency of 0.1 rpm
Adsorption to desorption segment ratio	2:1	Adsorption and desorption time of 400 and 200 s, respectively
Working capacity of Zeolite 13X (temperature swing between 40 and 150 °C)	1.22 mol/kg	Based on the isotherm reported by Mohammadi (2017) and assuming regeneration in a pure CO_2 environment
Diameter of the rotary wheel	2 m	Chosen so that the wheel fits inside a standard shipping container (Mr. Box, 2018)
Isosteric heat of CO_2 adsorption on Zeolite 13X	37,000 J/mol	Cavenati et al. (2004)
Specific heat of Zeolite 13X	920 J/(kg K)	Dantas et al. (2011)
Specific heat of the support material (Al)	900 J/(kg K)	Chase (1998)
Channels per unit area	741 channels per square inch	Mohammadi (2017)

Results	
Fraction of the total CO_2 captured by the TSA unit	~0.40
Total amount of adsorbent to be coated	738 kg
Length of the rotary wheel	1.556 m
Thermal power input required to heat the adsorbent	124.5 kW
Thermal power input required to supply heat of adsorption	55.51 kW
Thermal power input required to heat the support material	270.1 kW
Total thermal power input required for capturing all the CO_2 from natural gas	450.1 kW
Thermal power available within the process at 180 °C	~400 kW

The results indicate that a significant fraction (~0.3-0.4) of the CO_2 emissions from a small-scale SMR unit could be captured making use of the excess heat inherently available in the system. The reforming temperature can be increased, if need be, to increase the excess heat by ~25 % (Figure 3). Another alternative to meet the energy shortfall is to employ a separate NG combustor. However, this would require additional unit operations to be added to the small-scale SMR unit. Conversely, increasing the reforming temperature would only require increasing the size of the existing unit operations and thus represents a more compact means of generating the extra energy. A detailed comparison of the two options in terms of their

respective energy efficiencies is however outside the scope of the present study. The length of the rotary wheel predicted by this assessment is small enough to fit inside a standard shipping container with dimensions of 2.84 m×2.35 m×2.39 m (internal length×internal width×internal height) (Mr. Box, 2018). The container-based design of the CO_2 capture unit would reduce the physical space requirement and the commissioning time. For the corrugated structure reported in Mohammadi (2017), the power required to heat the support material is expected to be the highest. A significant amount of energy penalty could be avoided, by directly extruding the adsorbent in the desired form. However, at the same time, there are also certain advantages of coating the adsorbent on to a conductive support material. The metallic layer aids the heat transfer during adsorption and desorption, due to its high thermal conductivity (Rezaei and Webley, 2010); this highlights the importance of process design in minimising the energy required for CO_2 capture.

7. Conclusions

Detailed energetic analysis of the small-scale SMR process has been reported in this article, mainly in reference to carbon capture. Due to unavailability of cheap means of CO_2 transport, carbon capture from small-scale SMR process has been deemed economically infeasible and hence, not investigated much from a technical perspective. In this article, we have addressed this research gap by systematically analysing a generic, small-scale SMR process from the energetic and exergetic point of view. Small-scale SMR plants differ from large-scale SMR plants, mainly in terms of operating parameters and the fact that they are not usually integrated with other processes. SMR plants have an excess heat available within the process, which is generally used to produce export steam in large-scale SMR plants. In small-scale SMR plants, there is the potential to utilise this excess heat to capture a part of the CO_2 emitted from the process. GCCs for the small-scale SMR process have been used in this work to estimate the amount of excess heat available at different temperature levels. The reforming temperature has been identified as a critical process parameter influencing the amount of excess heat that can be extracted from the process. An increase in reforming temperature from 750 to 850 °C, increases the amount of excess heat available at 180 °C by about 28.4 %; this is accompanied by a relatively small decrease in the thermal and exergetic efficiency of about 1.62 and 1.09 %, respectively. Almost half of the CO_2 emissions can be captured at a high partial pressure, through energy imported from outside the process; a preliminary assessment shows that the remaining 30 to 40 % of the total CO_2 emissions can be captured by using the excess heat from within the process. The additional CO_2 has been assumed to be captured from reformer flue gas through a compact, structured adsorbent-based TSA process. Such encouraging results necessitate the need to further investigate structured adsorbent-based processes, through detailed process models; this should be the subject matter of further research.

8. Acknowledgements

The authors would like to acknowledge the financial support from Engineering and Physical Sciences Research Council, under grant no. EP/N024613/1.

References

Abanades, J.C., Arias, B., Lyngfelt, A., Mattisson, T., Wiley, D.E., Li, H., Ho, M.T., Mangano, E., Brandani , S., 2015. Emerging CO_2 capture systems. *International Journal of Greenhouse Gas Control, 40*, 126-166. doi: 10.1016/j.ijggc.2015.04.018

Air Liquide, 2015. *Press release.* Retrieved from: https://www.airliquide.com/sites/airliquide.com/files/2015/11/05/world-premiere_air-liquide-inaugurates-its-co2-cold-capture-system-cryocap.pdf (accessed 05/08/2018)

Air Products and Chemicals, Inc., 2018. *PRISM® Hydrogen Generators*. Retrieved from: http://www.airproducts.com/Microsites/phg.aspx (accessed: 12/12/2018)

Baade, W., Farnand, S., Hutchinson, R., Welch, K., 2012. CO_2 capture from SMRs: A demonstration project. *Hydrocarbon Processing*. September Issue, 63-68.

Boot-Handford, M.E., Abanades, J.C., Anthony, E.J., Blunt, M.J., Brandani , S., Mac Dowell, N.M., Fernández, J.R., Ferrari, M.C., Gross, R., Hallett, J.P., Haszeldine, R.S., Heptonstall, P.,Lyngfelt, A., Makuch, Z., Mangano, E., Porter, R.T.J., Pourkashanian, M., Rochelle, G.T., Shah, N., Yao, J.G., Fennell, P.S., 2014. Carbon capture and storage update. *Energy & Environmental Science, 7*(1), 130-189. doi: 10.1039/C3EE42350F

Cap-Op Energy, 2015. *Offset Project Plan for the Quest Carbon Capture and Storage Project*. Retrieved from: https://www.csaregistries.ca/files/projects/7306_8118_AEOR_OffsetProjectPlan_20150823_20350822.pdf (accessed 05/08/2018)

Cavenati, S., Grande, C. A., Rodrigues, A. E., 2004. Adsorption Equilibrium of Methane, Carbon Dioxide and Nitrogen on Zeolite 13X at High Pressures. *Journal of Chemical and Engineering Data*, 49(4), 1095-1101. doi: 10.1021/je0498917

Chase, M., 1998. *NIST-JANAF Thermochemical Tables* (4th ed.). American Institute of Physics.

Collodi, G., Azzaro, G., Ferrari, N., Santos, S., 2017. Techno-Economic Evaluation of Deploying CCS in SMR Based Merchant H_2 Production with NG as Feedstock and Fuel. *Energy Procedia, 114*, 2690-2712. doi: 10.1016/j.egypro.2017.03.1533

Committee on Climate Change (UK), 2017. *2017 Report to Parliament – Meeting Carbon Budgets: Closing the policy gap.* Retrieved from: https://www.theccc.org.uk/wp-content/uploads/2017/06/2017-Report-to-Parliament-Meeting-Carbon-Budgets-Closing-the-policy-gap.pdf (accessed 05/08/2018)

CORDIS, 2015. *Final Report Summary - HY2SEPS-2 (Hybrid Membrane - Pressure Swing Adsorption (PSA) Hydrogen Purification Systems).* Retrieved from: https://cordis.europa.eu/project/rcn/101420/reporting/en (accessed 18/03/2019)

Dantas, T., Luna, F., Silva Jr., I., Torres, A., Azevedo, D., Rodrigues, A., Moreira, R., 2011. Modelling of the fixed-bed adsorption of carbon dioxide and a carbon dioxide-nitrogen mixture on Zeolite 13X. *Brazillian Journal of Chemical Engineering*, *28*(03), 533-544. doi: 10.1590/S0104-66322011000300018

Department for Business, 2018. *Final UK greenhouse gas emissions national statistics: 1990-2016.* Retrieved from: https://www.gov.uk/government/uploads/system/uploads/attachment_data/file/679334/2016_Final_Emissions_Statistics_one_page_summary.pdf (accessed: 05/08/2018)

Department of Energy (US), 2013. *Report of the Hydrogen Production Expert Panel: A Subcommittee of the Hydrogen and Fuel Cell Technical Advisory Committee.* Retrieved from: https://www.hydrogen.energy.gov/pdfs/hpep_report_2013.pdf (accessed: 05/08/2018)

Ekins, P., Hawkins, S., Hughes, N., 2010. Hydrogen Technologies and Costs. In P. Ekins (Ed.), *Hydrogen Energy: Economic and Social Challenges*, 29-58. London: Earthscan.

FCH JU, 2013. *Fuel Cells and Hydrogen Joint Undertaking Programme Review 2012 (Final Report).* Retrieved from: https://www.fch.europa.eu/sites/default/files/FCH%20JU%20programme%20review%20final%20report%202012_0.pdf (accessed: 18/03/2019)

Grover, B., 2012. *Zero steam export with CO_2 recovery in a high thermal efficiency hydrogen plant.* US Patent No. 8,124,049 B2

H_2 Tools., 2013. *Hydrogen Tools.* Retrieved from: https://h2tools.org/sites/default/files/imports/files//Europe_merchant_hydrogen_plants_112015.xlsx (accessed: 05/08/2018)

Hajjaji, N., Pons, M.-N., Houas, A., Renaudin, V., 2012. Exergy analysis: An efficient tool for understanding and improving hydrogen production via the steam methane reforming process. *Energy Policy, 42*, 392-399. doi: 10.1016/j.enpol.2011.12.003

Hamelinck, C., Faaij, A., 2002. Future prospects for production of methanol and hydrogen from biomass. *Journal of Power Sciences, 111*, 2-22. doi: 10.1016/S0378-7753(02)00220-3

IEA-HIA, 2012. IEA-HIA Task 23 Small-scale Reformers for On-site Hydrogen Supply, *International Energy Agency.* Retrieved from: http://ieahydrogen.org/pdfs/Task23_Final-Report_ISBN.aspx (accessed: 05/08/2018)

IEA-HIA, 2006. Hydrogen Production and Storage: R&D Priorities and Gaps, *International Energy Agency.* Retrieved from: https://www.iea.org/publications/freepublications/publication/hydrogen.pdf (accessed: 05/08/2018)

Lemus, R. G., Duart, J. M., 2010. Updated hydrogen production costs and parities for conventional and renewable technologies. *International Journal of Hydrogen Energy*, 35(9), 3929-3936. doi: 10.1016/j.ijhydene.2010.02.034

Maxwell, G. R., 2005. Hydrogen Production. In *Synthetic Nitrogen Products: A Practical Guide to the Products and Processes*, 57-90. New York: Kluwer Academic Publishers (Springer Science + Business Media, Inc.).

Meerman, J., Hamborg, E., Keulen, T. V., Ramirez, A., Turkenburg, W., Faaij, A., 2012. Techno-economic assessment of CO_2 capture at steam methane reforming facilities using commercially available technology. *International Journal of Greenhouse Gas Control, 9*, 160-171. doi: 10.1016/j.ijggc.2012.02.018

Miller, R. J., 2016. The air we breathe; the fuel we burn. *Innovation*, May/June Issue, 17-20.

Mitsubishi Kakoki Kaisha, Ltd., 2018. *HyGeia : Small-Scale On-Site Hydrogen Generator*. Retrieved from: http://www.kakoki.co.jp/english/products/p-001/index.html (accessed: 05/08/2018)

Mohammadi, N., 2017. CO_2 capture from flue gas by a PSA process using a novel structured adsorbent. *Doctoral Thesis*. The University of South Carolina

Mr. Box., 2018. *Shipping Containers*. Retrieved from: https://www.mrbox.co.uk/shipping-containers/ (accessed: 05/08/2018)

Northern Gas Networks, 2016. *H21 Leeds City Gate*. Retrieved from: https://www.northerngasnetworks.co.uk/wp-content/uploads/2017/04/H21-Report-Interactive-PDF-July-2016.compressed.pdf (accessed: 05/08/2018)

Ogden, J. M., 2001. *Review of small stationary reformers for hydrogen production.* International Energy Agency.

Rezaei, F., Webley, P., 2010. Structured adsorbents in gas separation processes. *Separation and Purification Technology, 70(3)*, 243-256. doi: 10.1016/j.seppur.2009.10.004

Ruthven, D.M., Thaeron, C., 1997. Performance of a parallel passage adsorbent contactor. *Separation and Purification Technology, 12*, 43-60. doi: 10.1016/S1383-5866(97)00016-6

Schjolberg, I., Hulteberg, C., Yasuda, I., Nelsson, C., 2012. Small scale reformers for on-site hydrogen supply. *Energy Procedia*, 559-566. doi: 10.1016/j.egypro.2012.09.065

Shi, W., Yang, H., Shen, Y., Fu, Q., Zhang, D., Fu, B., 2018. Two-stage PSA/VSA to produce H_2 with CO_2 capture via steam methane reforming (SMR). *International Journal of Hydrogen Energy*, 43, 19057-19074. doi: 10.1016/j.ijhydene.2018.08.077

Silva, B., Solomon, I., Ribeiro, A.M., Lee, U-H., Hwang, Y. K., Chang, J-S, Loureiro, J.M., Rodrigues, A.E., 2013. H_2 purification by pressure swing adsorption using CuBTC. *Separation and Purification Technology*, 118, 744-756. doi: 10.1016/j.seppur.2013.08.024

Simpson, A. P., Lutz, A. E., 2007. Exergy analysis of hydrogen production via steam methane reforming. *International Journal of Hydrogen Energy, 32(18)*, 4811-4820. doi: 10.1016/j.ijhydene.2007.08.025

Sircar, S., Golden, T., 2000. Purification of Hydrogen by Pressure Swing Adsorption. *Separation Science and Technology*, 35(5), 667-687. doi: 10.1081/SS-100100183

Soltani, R., Rosen, M., Dincer, I., 2014. Assessment of CO_2 capture options from various points in steam methane reforming for hydrogen production. *International Journal of Hydrogen Energy, 39*(35), 20266-20275. doi: 10.1016/j.ijhydene.2014.09.161

Tanaka, Y., Sawada, Y., Tanase, D., Tanaka, J., Shiomi, S., Kasukawa, T., 2017. Tomakomai CCS Demonstration Project of Japan, CO_2 Injection in Process. *Energy Procedia, 114*, 5836-5846. doi: 10.1016/j.egypro.2017.03.1721

The Linde Group, 2018. *HYDROPRIME On-Site Hydrogen Generators*. Retrieved from: https://www.linde-gas.com/en/products_and_supply/electronic_gases_and_chemicals/on_site_gas_generation/hydroprime-on-site-hydrogen-generation/index.html (accessed: 12/12/2018)

Wagner, J.L., 1969. *Selective Adsorption Process*. US Patent No. 3,430,418.